Reactivities of a Bis(alkylidene) Complex. Synthesis of a Silyl Bis(alkylidyne) Complex and a Reaction Cycle among Symmetric Bis(alkylidyne), Bis(alkylidene), and Nonsymmetric Bis(alkylidyne) Compounds

Xiaozhan Liu,[†] Liting Li,[†] Jonathan B. Diminnie,[†] Glenn P. A. Yap,[‡]
Arnold L. Rheingold,[‡] and Ziling Xue*,[†]

Department of Chemistry, The University of Tennessee, Knoxville, Tennessee 37996-1600, and
Department of Chemistry & Biochemistry, The University of Delaware,
Newark, Delaware 19716-2522

Received July 29, 1998

An unstable bis(alkylidene) complex $(RCH_2)_4Ta_2({=}CHR)_2(Cl)_2$ (R = $SiMe_3$, **1**), prepared by the addition of 2 equiv of HCl to a symmetrically bridging bis(alkylidyne) complex $(RCH_2)_4Ta_2(\mu\text{-}CR)_2$ (**2a**), decomposes through elimination of $SiMe_4$ to form an unstable alkylidene−alkylidyne complex $(RCH_2)_3Ta_2({=}CHR)({\equiv}CR)(Cl)_2$ (**3**). This conversion of an alkylidene to alkylidyne ligand was found to follow first-order kinetics with $\Delta H_1^{\ddagger} = 14.1(0.8)$ kcal/mol and $\Delta S_1^{\ddagger} = -12(3)$ eu. This is, to our knowledge, the second reported kinetic study of alkylidene → alkylidyne conversion, and the kinetics of this conversion is in contrast to that of $(RCH_2)_3Ta{=}CHR \rightarrow (RCH_2)_4Ta_2(\mu\text{-}CR)_2$ (**2a**) reported earlier. Substitution of the chlorides by SiR_3^- (R = $SiMe_3$) leads to a preferential elimination of $HSiR_3$ and formation of the first silyl bis(alkylidyne) complex $(RCH_2)(R_3Si)Ta(\mu\text{-}CR)_2Ta(CH_2R)_2$ (**4**). Addition of excess PMe_3 to **1** produces a novel 1,1′-dimetallacyclobutadiene derivative $(Me_3P)_2(Cl)Ta(\mu\text{-}CR)_2Ta(Cl)(CH_2R)_2$ (**5a**) with two nonsymmetrically bridging alkylidyne ligands. Both bridging ligands coordinate with C=Ta double bonds to the same metal atom (and with C−Ta single bonds to the other metal atom). The two bridging alkylidyne ligands in **5a**, which are coordinated to one metal atom in the axial and equatorial position, respectively, are involved in an intramolecular ligand exchange. The kinetic barriers for this exchange were determined to be $\Delta H_2^{\ddagger} = 13.6(0.4)$ kcal/mol and $\Delta S_2^{\ddagger} = -5(2)$ eu in **5a**, and $\Delta H_3^{\ddagger} = 13.0(0.3)$ kcal/mol and $\Delta S_3^{\ddagger} = -5(1)$ eu in **5b**. Addition of 2 equiv of RCH_2Li to replace the Cl ligands in **5a** converts **5a** to **2a**, completing a reaction cycle **2a** → **1** → **5a** → **2a**. $(Me_3P)_2(RCH_2)Ta(\mu\text{-}CR)_2Ta(Cl)(CH_2R)_2$ (**6**) was identified as an intermediate in the conversion of **5a** to **2a**.

Introduction

Early-transition-metal silyl complexes have been intensively studied for their unique bonding, structure, and catalytic activities in processes such as polysilane synthesis.[1] Most known silyl complexes of groups 4−6 contain cyclopentadienyl (Cp) or analogous anionic π-ligands[2] or other supporting ligands such as CO, phosphines, or alkoxides to alleviate electron deficiency in these silyl complexes.[3] We recently reported a new type of early-transition-metal silyl complexes free of such supporting ligands.[4] These complexes $(Me_3ECH_2)_3M{-}Si(SiMe_3)_3$ (M = Ti, Zr; E = C, Si), $(Me_3ECH_2)_2Ta({=}CHEMe_3)SiR_3$ [$R_3 = (SiMe_3)_3$, $Ph_2{}^tBu$], and $(Me_3CCH_2)_3W({\equiv}CCMe_3)Si(SiMe_3)_3$ are silyl analogues of the archetypical alkyl [$(Me_3ECH_2)_4M$], alkylidene [$(Me_3ECH_2)_3Ta{=}CHEMe_3$], and alkylidyne [$(Me_3ECH_2)_3W{\equiv}CEMe_3$] complexes.[4] We subsequently attempted the synthesis of Cp-free dinuclear silyl alkyli-

---

[†] The University of Tennessee.

[‡] The University of Delaware.

(1) For recent reviews, see: (a) Tilley, T. D. In *The Silicon-Heteroatom Bond*; Patai, S., Rappoport, Z., Eds.; Wiley: New York, 1991, Chapters 9 and 10, pp 245, 309. (b) Sharma, H. K.; Pannell, K. H. *Chem. Rev.* **1995**, *95*, 1351. (c) Schubert, U. *Transition Met. Chem.* **1991**, *16*, 136. (d) Schubert, U. *Adv. Organomet. Chem.* **1990**, *30*, 151. (e) Schubert, U. *Angew. Chem., Int. Ed. Engl.* **1994**, *33*, 419, and references therein.

(2) See, for example: (a) Aitken, C. T.; Harrod, J. F.; Samuel, E. *J. Am. Chem. Soc.* **1986**, *108*, 4059. (b) Woo, H.-G.; Heyn, R. H.; Tilley, T. D. *J. Am. Chem. Soc.* **1992**, *114*, 5698. (c) Jiang, Q.; Pestana, D. C.; Carroll, P. J.; Berry, D. H. *Organometallics* **1994**, *13*, 3679. (d) Kreutzer, K. A.; Fisher, R. A.; Davis, W. M.; Spaltenstein, E.; Buchwald, S. L. *Organometallics* **1991**, *10*, 4031. (e) Corey, J. Y.; Zhu, X.-H. *J. Organomet. Chem.* **1992**, *439*, 1. (f) Kingston, B. M.; Lappert, M. F. *J. Chem. Soc., Dalton Trans.* **1972**, 69. (g) Schubert, U.; Schenkel, A. *Chem. Ber.* **1988**, *121*, 939. (h) Parkin, G.; Bunel, E.; Burger, B. J.; Trimmer, M. S.; Van Asselt, A.; Bercaw, J. E. *J. Mol. Catal.* **1987**, *41*, 21. (i) Hengge, E.; Weinberger, M. *J. Organomet. Chem.* **1992**, *433*, 21. (j) Takahashi, T.; Hasegawa, M.; Suzuki, N.; Saburi, M.; Rousset, C. J.; Fanwick, P. E.; Negishi, E. *J. Am. Chem. Soc.* **1991**, *113*, 8564. (k) For a more complete list, see reviews in ref 1.

(3) For example: (a) $(dppe)(CO)_3M(H)SiR_3$ (M = Cr, Mo, W): Schubert, U.; Kirchgässner, U.; Grönen, J.; Piana, H. *Polyhedron* **1989**, *8*, 1589. (b) $({}^tBuO)_3MSi(SiMe_3)_3$ (M = Zr, Hf): Heyn, R. H.; Tilley, T. D. *Inorg. Chem.* **1989**, *28*, 1768. See refs 1 and 4 for a more complete list.

(4) (a) Xue, Z. *Comments Inorg. Chem.* **1996**, *18*, 223. (b) Xue, Z.; Li, L.; Hoyt, L. K.; Diminnie, J. B.; Pollitte, J. L. *J. Am. Chem. Soc.* **1994**, *116*, 2169. (c) Li, L.; Diminnie, J. B.; Liu, X.; Pollitte, J. L.; Xue, Z. *Organometallics* **1996**, *15*, 3520. (d) Diminnie, J. B.; Hall, H. D.; Xue, Z. *J. Chem. Soc., Chem. Commun.* **1996**, 2383. (e) McAlexander, L. H.; Hung, M.; Li, L.; Diminnie, J. B.; Xue, Z.; Yap, G. P. A.; Rheingold, A. L. *Organometallics* **1996**, *15*, 5231. (f) Diminnie, J. B.; Xue, Z. *J. Am. Chem. Soc.* **1997**, *119*, 12657. (g) Wu, Z.; Diminnie, J. B.; Xue, Z. *Organometallics* **1998**, *17*, 2917.

S0276-7333(98)00652-9 CCC: $15.00
Publication on Web 09/12/1998

dyne complexes; such early-transition-metal complexes have not yet been reported. A new bis(alkylidene) complex $(RCH_2)_4Ta_2(=CHR)_2(Cl)_2$ (R = $SiMe_3$, **1**) and a new alkylidene alkylidyne complex $(RCH_2)_3Ta_2(=CHR)(\equiv CR)(Cl)_2$ (**3**) were prepared as starting materials. **3** was found to react with 2 equiv of $Li(THF)_3SiR_3$ (R = $SiMe_3$) to give a dinuclear silyl complex $(R_3Si)(RCH_2)Ta(\mu\text{-}CR)_2Ta(CH_2R)_2$ (**4**), while **1** reacts with 2 equiv of $Li(THF)_3SiR_3$ to give $(RCH_2)_4Ta_2(\mu\text{-}CR)_2$ (**2a**). **4** is the silyl analogue of **2a**, one of the first reported high-oxidation-state alkylidyne complexes.

We also discovered that, in the absence of added SiR_3^-, the alkylidene ligand in **1** undergoes an alkane elimination to give an alkylidyne ligand in **3**. The mechanistic pathways in the formation of archetypal alkylidyne complexes $(Me_3ECH_2)_3M\equiv CEMe_3$ (E = C, Si; M = Mo, W) are, to our knowledge, unknown. α-Hydrogen abstraction is believed to be involved in the conversion of an alkyl ligand (through an alkylidene) to the alkylidyne ligand in $(RCH_2)_3M\equiv CR$.[5] The conversion from **1** to **3** offered a unique chance to study in detail the conversion of an alkylidene to alkylidyne ligand.

Bridging bis(alkylidyne) ligands are normally observed in coordinatively unsaturated complexes.[5] Such bridging ligands usually adopt symmetric bonding to the two metal atoms as in $(RCH_2)_2M(\mu\text{-}CR)_2M(CH_2R)_2$ (M = Ta, **2a**; Nb, **2b**; W).[6,7] Complexes with nonsymmetrically bridging bis(alkylidyne) ligands are rarely seen and, to our knowledge, have only been reported in $W_2(RCH_2)_4(\mu\text{-}CR)_2(\eta^2\text{-}PhC_2Me)$.[8] In an attempt to stabilize **1**, we found that **1** reacts with PMe_3 to give $(Me_3P)_2ClTa(\mu\text{-}CR)_2Ta(Cl)(CH_2R)_2$ (**5a**) containing such unusual nonsymmetrically bridging bis(alkylidyne) ligands.

We report here our kinetic studies of the conversion of an alkylidene ligand in **1** to an alkylidyne ligand in **3**, syntheses of the first structurally characterized d^0 silyl alkylidyne complex **4** and the novel 1,1′-dimetallacyclobutadiene derivatives **5a**,**b**, and an unusual reaction cycle among symmetric bis(alkylidyne) **2a**,**b**, bis(alkylidene) **1**, nonsymmetric bis(alkylidyne) **5a**,**b**, and **6**. Preliminary results about this reaction cycle have been reported.[9]

Experimental Section

All manipulations, unless noted, were performed under a dry nitrogen atmosphere with the use of either a drybox or standard Schlenk techniques. All solvents were purified by distillation from potassium/benzophenone ketyl. Benzene-d_6 and toluene-d_8 were dried over activated molecular sieves and stored under N_2. NMR spectra, unless noted, were recorded at 23 °C on a Bruker AC-250 or AMX-400 Fourier transform spectrometer and referenced to solvents (residual protons in the ^1H spectra). $(RCH_2)_2M(\mu\text{-}CR)_2M(CH_2R)_2$ (M = Ta, **2a**; Nb, **2b**),[6] $Li(THF)_3SiR_3$,[10] $Li(THF)_2SiPh_2{}^tBu$,[11] and $LiCH_2R$[12] were prepared by the literature procedures. HCl in Et_2O (1.0 M, Aldrich), $ClSiPh_2{}^tBu$ (Aldrich), and Li wire (high Na content, Aldrich) were used as received. Elemental analyses were performed by E+R Microanalytical Laboratory, Corona, NY (for **4**) and Desert Analytics, Tucson, AZ (for **5a**, **5b**, and $^tBuPh_2SiSiPh_2{}^tBu$).

For the kinetic studies, the rate constants were obtained from at least two separate experiments at a given temperature, and their averages are listed. The *maximum* random uncertainty in the rate constants was combined with the estimated systematic uncertainty, ca. 5%.[13] The total uncertainties in the rate constants were used in the Eyring plots and error propagation calculations. The estimated uncertainty in the temperature measurements for an NMR probe was 1 K. The activation enthalpies ($\Delta H^\ddagger$) and entropies ($\Delta S^\ddagger$) were calculated from an unweighted nonlinear least-squares procedure contained in the SigmaPlot Scientific Graph System, which is available from Jandel Corporation. The uncertainties in $\Delta H^\ddagger$ and $\Delta S^\ddagger$ were computed from the error propagation formulas derived from the Eyring equation by Girolami and co-workers.[14]

Preparation of $(RCH_2)_4(Cl)_2Ta_2(=CHR)_2$ (1). This unstable compound was prepared by the addition of 0.113 mL of HCl (1.0 M in Et_2O) to 50 mg of **2a** (0.057 mmol) in Et_2O (1 mL) at −78 °C. The color of the solution changed from red to yellow during the formation of the product. The compound was found to decompose above −50 °C, and was identified by ^1H, ^{13}C, and $^1H-^{13}C$ heteronuclear correlation (HETCOR) spectroscopy. ^1H NMR (toluene-d_8, 400.1 MHz, −50 °C): δ 5.57 (s, 2H, $CH=$), 2.50 (d, 2H, CH_aH_b, $^2J_{H-H}$ = 12 Hz), 2.04 (d, 2H, CH_cH_d, $^2J_{H-H}$ = 12 Hz), 1.68 (d, 4H, CH_aH_b, CH_cH_d), 0.40 (s, 18H, $Me_3SiCH=$), 0.34 (s, 18H, Me_3SiCH_2), 0.30 (s, 18H, Me_3SiCH_2). ^{13}C NMR (toluene-d_8, 100.6 MHz, −50 °C): δ 250.93 ($CH=$, $^1J_{C-H}$ = 92.0 Hz), 100.47 (CH_aH_b, $^1J_{C-H}$ = 108.1 Hz), 92.28 (CH_cH_d, $^1J_{C-H}$ = 110.6 Hz), 3.08 ($Me_3SiCH=$, $^1J_{C-H}$ = 118.9 Hz), 2.33 (Me_3SiCH_2, $^1J_{C-H}$ = 119.2 Hz), 1.91 (Me_3SiCH_2, $^1J_{C-H}$ = 118.8 Hz).

Reaction of 1 with 2 equiv of $Li(THF)_3SiR_3$. Complex **1** was prepared by adding 0.50 mL of HCl (1.0 M in Et_2O, 0.50 mmol) to a solution of $(RCH_2)_4Ta_2(\mu\text{-}CR)_2$ (**2a**, 222 mg, 0.25 mmol) in Et_2O (3 mL) at −78 °C. A solution of $Li(THF)_3SiR_3$ (237 mg, 0.50 mmol) in Et_2O (2 mL) was then added to the yellow solution at −78 °C. The solution turned dark and then changed to orange-red after the solution was slowly warmed to −30 °C. NMR spectra showed the products were **2a**, $HSiR_3$, and a small amount of R_3SiSiR_3.[15]

Reaction of 1 with 2 equiv of $Li(THF)_2SiPh_2{}^tBu$. Complex **1** (0.104 mmol) at −78 °C was prepared from 92.0 mg of **2a** (0.104 mmol) in Et_2O (1 mL) and 0.21 mL of HCl (1.0 M in Et_2O, 0.21 mmol). $Li(THF)_2SiPh_2{}^tBu$ (82 mg, 0.21 mmol) in Et_2O (1 mL) was then added to the yellow solution of **1** at −78 °C. The solution turned dark green immediately and then to orange-red after the solution was slowly warmed to −35 °C. NMR spectra at room temperature showed the products were **2a**, $HSiPh_2{}^tBu$, and a small amount of $^tBuPh_2SiSiPh_2{}^tBu$.

---

[5] See, for example: (a) Fischer, H.; Hoffman, P.; Kreissl, F. R.; Schrock, R. R.; Schubert, U.; Weiss, K. *Carbyne Complexes*; VCH: New York, 1988. (b) Schrock, R. R. *Acc. Chem. Res.* **1986**, *19*, 342. (c) Nugent, W. A.; Mayer, J. M. *Metal−Ligand Multiple Bonds*; Wiley: New York, 1988. (d) Mayr, A.; Hoffmeister, H. *Adv. Organomet. Chem.* **1991**, *32*, 227. (e) Feldman, J.; Schrock, R. R. *Prog. Inorg. Chem.* **1991**, *39*, 1.

[6] (a) Mowat, W.; Wilkinson, G. *J. Chem. Soc., Dalton Trans.* **1973**, 1120. (b) Huq, F.; Mowat, W.; Skapski A. C.; Wilkinson, G. *J. Chem. Soc., Chem. Commun.* **1971**, 1477.

[7] See, e.g.: (a) Fanwick, P. E.; Ogilvy, A. E.; Rothwell, I. P. *Organometallics* **1987**, *6*, 73. (b) Chisholm, M. H.; Heppert, J. A.; Huffman, J. C. *J. Am. Chem. Soc.* **1984**, *106*, 1151, and references therein.

[8] Chisholm, M. H.; Huffman, J. C.; Heppert, J. A. *J. Am. Chem. Soc.* **1985**, *107*, 5116.

[9] See this communication for an ORTEP view of **5a**: Li, L.; Xue, Z.; Yap, G. P. A.; Rheingold, A. L. *Organometallics* **1995**, *14*, 4992.

[10] Gutekunst, G.; Brook, A. G. *J. Organomet. Chem.* **1982**, *225*, 1.

[11] Campion, B. K.; Heyn, R. H.; Tilley, T. D. *Organometallics* **1993**, *12*, 2584.

[12] Tessier-Youngs, C.; Beachley, O. T., Jr. *Inorg. Synth.* **1986**, *24*, 95.

[13] (a) Li, L.; Hung, M.; Xue, Z. *J. Am. Chem. Soc.* **1995**, *117*, 12746. (b) Li, L. Ph.D. Thesis, The University of Tennessee, Knoxville, 1996.

[14] Morse, P. M.; Spencer, M. D.; Wilson, S. R.; Girolami, G. S. *Organometallics* **1994**, *13*, 1646.

[15] Heine, A.; Herbst-Irmer, R.; Sheldrick, G. M.; Stalke, D. *Inorg. Chem.* **1993**, *32*, 2694.

Chart 1. Labeling Scheme for 3-C

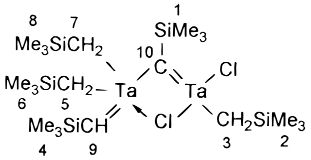

Preparation of $^tBuPh_2SiSiPh_2{}^tBu$.[16] To confirm the formation of $^tBuPh_2SiSiPh_2{}^tBu$ in the previous reaction, this compound was prepared and characterized independently. A solution of $ClSiPh_2{}^tBu$ (8.0 mL, 8.5 g, 30.9 mmol) and THF (20 mL) was added to Li (0.117 g of cut wire, 16.9 mmol) suspended in 20 mL of THF under Ar at 23 °C. The solution turned red-yellow immediately and then colorless in 3 h. After stirring overnight, the solution was filtered to obtain the product as a white solid (5.0 g). The volatiles in the supernatant solution, which contained the remaining product, were removed in vacuo. The oily solid mixture was first washed with a small amount of hexane to remove the unreacted $ClSiPh_2{}^tBu$. The solid mixture was then extracted with toluene and recrystallized to yield an additional 1.8 g (total 6.8 g, 92% yield based on $ClSiPh_2{}^tBu$). ^1H NMR (benzene-d_6, 250.1 MHz): δ 7.85−7.82 (m, 4H, Ph), 7.16−7.11 (m, 6H, Ph), 0.98 (s, 9H, Me_3C). $^{13}C\{^1H\}$ (benzene-d_6, 62.9 MHz): δ 137.88 (Ph), 137.00 (Ph), 129.14 (Ph), 127.73 (Ph), 29.44 (Me_3C), 20.64 (Me_3C). Anal. Calcd for $C_{32}H_{38}Si_2$: C, 80.29; H, 8.01. Found: C, 80.14; H, 8.01.

Preparation of $(RCH_2)_3Ta_2({=}CHR)({\equiv}CR)(Cl)_2$ (3).[4b] **2a** (0.111 g, 0.126 mmol) was weighed into a Schlenk flask and dissolved in Et_2O. HCl (0.252 mL, 1.0 M in Et_2O, 0.252 mmol) was then added to the solution of **2a** at −50 °C with vigorous stirring. The resulting solution of **1** was warmed to −28 °C and held at this temperature for 1 h. The solvent was then removed, and the thermally unstable solid **3** was dissolved in toluene-d_8 and characterized by ^1H and ^{13}C NMR, $^1H-^{13}C$ HETCOR, long-range HETCOR, and NOESY. ^1H NMR (toluene-d_8, −45 °C, 400.1 MHz; see Chart 1 for labeling scheme and Discussion for the structure of **3**): δ 4.68 (s, 1H, H_9), 1.93 [d, 1H, $H_{3a,}$ $2J(H_{3a}-H_{3b}) = 12.8$ Hz], 1.91 [d, 1H, H_{5a}, $^2J(H_{5a}-H_{5b}) = 10.4$ Hz], 1.79 (d, 1H, H_{5b}), 1.44 [d, 1H, H_{7a}, $^2J(H_{7a}-H_{7b}) = 13.6$ Hz], 1.13 (d, 1H, H_{3b}), 1.00 (d, 1H, H_{7b}), 0.42 (s, 9H, H_4], 0.36 (s, 18H, H_2 and H_6), 0.34 (s, 9H, H_1), 0.21(s, 9H, H_8). $^{13}C\{^1H\}$ NMR (toluene-d_8, −45 °C, 100.6 MHz): δ 376.39 (C_{10}), 237.36 (C_9, $^1J_{C-H} = 104.3$ Hz), 91.51 (C_5, $^1J_{C-H} = 110.8$ Hz), 91.21 (C_3, $^1J_{C-H} = 108.3$ Hz), 78.29 (C_7, $^1J_{C-H} = 110.8$ Hz), 4.33 (C_4, $^1J_{C-H} = 120.4$ Hz), 3.52 (C_1, $^1J_{C-H} = 119.0$ Hz), 2.99 (C_6, $^1J_{C-H} = 118.9$ Hz), 2.11 (C_2 and C_8, $^1J_{C-H} = 119.4$ Hz).

Kinetic Study of the Conversion of 1 to 3. **2a** was weighed into a Schlenk flask and then dissolved in Et_2O. HCl (2 equiv) was added to the solution of **2a** at −50 °C with vigorous stirring to make **1**. After removal of the solvent, **1** was dissolved in precooled toluene-d_8, and the solution was transferred to an NMR tube containing 4,4′-dimethylbiphenyl (0.2 mg) as an internal standard. The initial concentrations of **1** ranged from 0.145 to 0.254 M, and the concentration of the internal standard was 0.219 M. The NMR spectra were taken at 244 ± 1, 238 ± 1, 233 ± 1, 227 ± 1, 222 ± 1, and 217 ± 1 K, respectively. The concentrations of **1** were calculated from the integrations of its ^1H NMR peaks with respect to that of the internal standard.

Preparation of $(RCH_2)(R_3Si)Ta(\mu\text{-}CR)_2Ta(CH_2R)_2$ (4). **1** was prepared by adding HCl/Et_2O solution (1.0 M, 3.46 mL) to a stirred solution of **2a** (1.18 g, 1.34 mmol) in Et_2O at −50 °C. The resulting solution of **1** was warmed to −35 °C, and held at this temperature for 12 h to complete the decomposition of **1** to dark red-brown **3**. The solvent was removed in vacuo, and the solid was dissolved in toluene. To this solution at −50 °C was added $LiSiR_3(THF)_3$ (1.40 g, 2.97 mmol). The reaction mixture was warmed to room temperature and stirred for 30 min. After filtration, the solution was concentrated and cooled to −30 °C to give 0.59 g (0.566 mmol, 42.3% yield based on **2a**) of **4** as maroon crystals. ^1H NMR (toluene-d_8, 400.1 MHz, 27 °C): δ 1.53 (s, 2H, CH_2SiMe_3), 1.00 (s, 2H, CH_2SiMe_3), 0.59 (s, 9H, Me_3Si), 0.51 [s, 27H, $(Me_3Si)_3Si$], 0.38 (s, 2H, CH_2SiMe_3), 0.30 (s, 9H, Me_3Si), 0.26 (s, 9H, Me_3Si), 0.15 (s, 18H, $2Me_3Si$). ^{13}C NMR (toluene-d_8, 100.6 MHz, 27 °C): δ 424.07 (${\equiv}CSiMe_3$), 107.40 (CH_2SiMe_3), 84.08 (CH_2SiMe_3), 79.04 (CH_2SiMe_3), 6.06 ($Me_3SiC{\equiv}$), 5.81 [$(Me_3Si)_3Si$], 4.38 (Me_3SiCH_2), 3.86 (Me_3SiCH_2), 3.64 (Me_3SiCH_2). ^{29}Si NMR (benzene-d_6, 79.5 MHz, 27 °C): δ 7.50 (CH_2SiMe_3), 4.05 (CH_2SiMe_3), 2.94 (CH_2SiMe_3), 0.00 [$Si(SiMe_3)_3$], −30.29 (${\equiv}CSiMe_3$), −35.85 [$Si(SiMe_3)_3$]. Anal. Calcd for $C_{29}H_{78}Si_9Ta_2$: C, 33.44; H, 7.55. Found: C, 33.20; H, 7.53.

Preparation of $(Me_3P)_2(Cl)Ta(\mu\text{-}CR)_2Ta(Cl)(CH_2R)_2$ (5a). To a solution of **2a** (2.0 g, 2.3 mmol) in Et_2O (15 mL) at −78 °C was slowly added HCl in Et_2O (1.0 M, 4.54 mL, 4.54 mmol) via syringe. The color changed from red to yellow. After the solution was stirred for 10 min, PMe_3 (0.6 mL, 6 mmol) was added at −78 °C. A yellow precipitate formed immediately. Recrystallization at −20 °C yielded 1.85 g of **5a** as yellow crystals (88% yield based on **2a**). **5a**, though thermally stable at 23 °C, was found to be light sensitive and should be kept in the dark. ^1H NMR (benzene-d_6, 250.1 MHz, 23 °C): δ 2.11 (d, 2H, CH_aH_b, $^2J_{H-H} = 12.4$ Hz, $^2J_{Si-H} = 8.3$ Hz), 1.39 (t, 18H, PMe_3, $^2J_{P-H} = 3.7$ Hz), 0.82 (d, 2H, CH_aH_b, $^2J_{H-H} = 12.4$ Hz, $^2J_{Si-H} = 8.3$ Hz), 0.45 (s, 18H, Me_3SiCH_2, $^2J_{Si-H} = 6.4$ Hz), 0.24 (broad, s, 9H, $Me_3SiC{\equiv}$), 0.11 (broad, s, 9H, $Me_3SiC{\equiv}$). $^{13}C\{^1H\}$ (benzene-d_6, 62.9 MHz, 23 °C): δ 408.49, 408.21 (broad, $C{\equiv}$), 78.46 (CH_2, $^1J_{C-H} = 107.3$ Hz, $^1J_{Si-C} = 42.0$ Hz), 16.44 (t, PMe_3, $^1J_{C-H} = 129.7$ Hz, $^1J_{P-C} = 12.3$ Hz), 5.57 ($Me_3SiC{\equiv}$), 3.27 (Me_3SiCH_2, $^1J_{C-H} = 118.4$ Hz, $^1J_{Si-C} = 44$ Hz). ^1H NMR (toluene-d_8, 400.1 MHz, −30 °C): δ 2.09 (d, 2H, CH_aH_b, $^2J_{H-H} = 12.6$ Hz), 1.35 (t, 18H, PMe_3, $^2J_{P-H} = 3.8$ Hz), 0.91 (d, 2H, CH_aH_b, $^2J_{H-H} = 12.6$ Hz), 0.49 (s, 18H, Me_3SiCH_2, $^2J_{Si-H} = 6$ Hz), 0.27 (s, 9H, $Me_3SiC{\equiv}$), 0.12 (s, 9H, $Me_3SiC{\equiv}$). $^{13}C\{^1H\}$ (toluene-d_8, 100.6 MHz, −30 °C): δ 408.61, 408.30 ($C{\equiv}$), 77.78 (CH_2, $^1J_{C-H} = 107.3$ Hz, $^1J_{Si-C} = 41$ Hz), 15.85 (t, PMe_3, $^1J_{C-H} = 130$ Hz, $^1J_{P-C} = 12$ Hz), 4.99, 4.74 ($Me_3SiC{\equiv}$, $^1J_{C-H} = 118.4$ Hz, $^1J_{Si-C} = 52$ Hz), 3.14 (Me_3SiCH_2 $^1J_{C-H} = 118.3$ Hz, $^1J_{Si-C} = 50$ Hz). Anal. Calcd for $C_{22}H_{58}Cl_2P_2Si_4Ta_2$: C, 28.42; H, 6.29. Found: C, 28.60; H, 6.29.

Reaction of 5a with 2 equiv of RCH_2Li. To a solution of **5a** (50 mg, 0.053 mmol) in benzene-d_6 (0.4 mL) was added a solution of RCH_2Li (10 mg, 0.106 mmol) in benzene-d_6 (0.4 mL) at room temperature. The solution turned red at once. The NMR spectra showed the products were **2a** and free PMe_3.

Identification of $(Me_3P)_2(RCH_2)Ta(\mu\text{-}CR)_2Ta(CH_aH_bR)_2(Cl)$ (6) in the reaction of 5a with RCH_2Li. Complex **5a** (25 mg, 0.0269 mmol) dissolved in toluene-d_8 (0.4 mL) at −10 °C was added to 5 mg of RCH_2Li (0.053 mmol) in toluene-d_8 (0.4 mL) at −60 °C. In the slow formation of **2a** at −50 °C, an intermediate **6** was identified by ^1H and ^{13}C NMR and $^1H-^{13}C$ HETCOR. ^1H NMR (toluene-d_8, 400.1 MHz, −50 °C): δ 2.18 (d, 2H, CH_aH_b, $^2J_{H-H} = 12.4$ Hz), 1.43 (t, 18H, PMe_3, $^2J_{P-H} = 3.3$ Hz), 0.77 (d, 2H, CH_aH_b), 0.55 (s, 18H, $CH_aH_bSiMe_3$), 0.23 (s, 9H, Me_3SiCH_2), 0.15 (s, 9H, $Me_3SiC{\equiv}$), 0.10 (s, 9H, $Me_3SiC{\equiv}$), −1.25 (t, 2H, CH_2, $^3J_{P-H} = 14.8$ Hz). ^{13}C NMR (toluene-d_8, 100.6 MHz, −50 °C): δ 406.92, 406.29 ($Me_3SiC{\equiv}$), 76.80 ($Me_3SiCH_aH_b$, $^1J_{C-H} = 106.7$ Hz), 46.54 (Me_3SiCH_2, $^1J_{C-H} = 98.0$ Hz), 17.64 (t, PMe_3, $^1J_{C-H} = 129.6$ Hz, $^1J_{P-C} = 12.1$ Hz), 5.69 (Me_3SiCH_2, $^1J_{C-H} = 116.6$ Hz), 5.64, 5.61 ($Me_3SiC{\equiv}$, $^1J_{C-H} = 116.6$ Hz), 3.32 ($CH_aH_bSiMe_3$, $^1J_{C-H} = 117.9$ Hz). **6** slowly reacted with the remaining RCH_2Li at −50 °C. When warmed to −20 °C, the reaction was completed within 20 min to give **2a**.

---

[16] Furstner, A.; Weidmann, H. *J. Organomet. Chem.* **1988**, *354*, 15.

Table 1. Crystal Data for 4, 5a, and 5b[a]

	4	**5a**	**5b**
formula	$C_{29}H_{78}Si_9Ta_2$	$C_{22}H_{58}Cl_2P_2Si_4Ta_2$	$C_{22}H_{58}Cl_2P_2Si_4Nb_2$
fw	1041.62	929.8	753.7
color	maroon	yellow	red
cryst syst	monoclinic	monoclinic	monoclinic
space group	$P2_1/c$	$P2_1/n$	$P2_1/n$
a (Å)	10.907(5)	10.668(2)	10.633(3)
b (Å)	18.112(6)	17.481(2)	17.411(5)
c (Å)	25.095(8)	20.962(3)	20.685(7)
β(deg)	97.53(3)	94.98(1)	94.24(2)
V (Å^3)	4915(3)	3894(1)	3819(2)
Z	4	4	4
d_{calcd} (g cm^{-3})	1.408	1.586	1.311
μ (cm^{-1})	46.86	59.68	9.60
temp (K)	173	245	173
2θ (deg)	3−45	4−50	3−45
no. of data collected	6907	6993	5343
no. of independent data	6465 ($R_{int} = 0.0451$)	6804 ($R_{int} = 0.0213$)	5024 ($R_{int} = 0.0181$)
no. of variables	361	290	463
refinement method (full-matrix least-squares on)	F^2	F	F^2
R (obs data)	0.0441	0.0339	0.0251
weighted R	0.1115 (wR2)	0.0430 (wR)	0.0876 (wR2)
GOF	0.913	0.99	0.836

[a] Structure of **5a** was determined at the University of Delaware, **4** and **5b** at the University of Tennessee.

Preparation of $(Me_3P)_2(Cl)Nb(\mu\text{-}CR)_2Nb(Cl)(CH_2R)_2$ (5b). HCl (1.0 M in Et_2O, 4.25 mL, 4.25 mmol) was added dropwise to a solution of $(RCH_2)_2Nb(\mu\text{-}CR)_2Nb(CH_2R)_2$ (**2b**, 1.50 g, 2.12 mmol) and PMe_3 (0.44 mL, 4.3 mmol) in diethyl ether (40 mL) at −78 °C with vigorous stirring. The solution was warmed to room temperature and stirred for 20 min. Cooling the solution to −20 °C afforded 0.64 g of **5b** as red crystals (0.85 mmol, 40% yield). **5b**, though thermally stable at room temperature, was found to be light sensitive and should be kept in the dark. ^1H NMR (toluene-d_8, 400.1 MHz, −60 °C): δ 2.95 (d, 2H, CH_aH_b, $^2J_{H-H} = 12.0$ Hz), 1.93 (d, 2H, CH_aH_b, $^2J_{H-H} = 12.0$ Hz), 1.26 (t, 18H, PMe_3, $^2J_{P-H} = 3.5$ Hz), 0.56 (s, 18H, Me_3SiCH_2), 0.30 (s, 9H, Me_3SiC), 0.12 (s, 9H, Me_3SiC). $^{13}C\{^1H\}$ NMR (toluene-d_8, 100.6 MHz, −60 °C): δ 428.40, 428.80 (broad, $C\equiv$), 69.86 (broad, CH_2, $^1J_{C-H} = 109.9$ Hz), 15.45 (t, PMe_3, $^1J_{P-C} = 11.1$ Hz, $^1J_{C-H} = 130.0$ Hz), 3.21 and 2.95 ($Me_3SiC\equiv$, $^1J_{C-H} = 119.0$ Hz), 2.87 (Me_3SiCH_2, $^1J_{C-H} = 118.7$ Hz). Anal. Calcd for $C_{22}H_{58}Cl_2P_2Si_4Nb_2$: C, 35.06; H, 7.76. Found: C, 34.90; H, 7.87.

Reaction of 5b with RCH_2Li. To a solution of **5b** (16.7 mg, 0.022 mmol) in benzene-d_6 (0.3 mL) was added RCH_2Li (4.1 mg, 0.044 mmol) in benzene-d_6 (0.3 mL) at room temperature. The solution turned cloudy at once and was filtered. The NMR spectra of the solution showed the products were **2b** and free PMe_3.

Kinetic Study of the Axial−Equatorial Alkylidyne Ligand Exchange in 5a and 5b. Complex **5a** (0.031−0.059 M in 0.46−0.52 mL) or **5b** (0.023−0.032 M in 0.57−0.63 mL) was dissolved in toluene-d_8 in an NMR tube. Variable-temperature NMR spectra were recorded on a Bruker AMX-400 spectrometer. Simulations of the dynamic NMR spectra were carried out with the use of the program DNMR.[14] The rates of exchange as a function of temperature were determined from visual comparisons of experimental spectra with computed trial line shapes.

X-ray Crystal Structure Determination of 4. The crystal structure of **4** was obtained at 173 K on a Siemens R3m/V diffractometer fitted with a Nicolet LT-2 low-temperature device. A suitable crystal of approximate dimensions 0.40 × 0.20 × 0.20 mm was cut from a larger crystal, coated in Paratone oil (Exxon), and mounted under a stream of nitrogen. The unit cell dimensions were calculated from the angular settings of 48 reflections located from a rotation photograph and an automatic peak search routine. **4** was found to crystallize in the monoclinic system. A total of 6907 reflections were collected using ω-scans, of which 6465 were determined to be unique. Corrections for Lorentz and polarization effects were made during data reduction, and an absorption correction based on ψ-scans collected on 5 reflections with $22° < 2\theta < 42°$ was applied to the data set. The |E*E−1| statistics, as well as the observed systematic absences in the data, were uniquely consistent with the space group $P2_1/c$. The structure was solved by direct methods using the Siemens SHELXTL 93 (version 5.0) proprietary software package, completed by successive Fourier syntheses, and refined to convergence by successive full-matrix least-squares refinements on F^2. All non-hydrogen atoms were anisotropically refined. Hydrogen atoms were placed in calculated positions and introduced into the refinement as fixed contributors with isotropic U values of 0.08 Å^2. Crystal, data collection, and refinement parameters are listed in Table 1.

X-ray Crystal Structure Determination of 5a. A suitable crystal was selected and mounted in a thin-walled, nitrogen-flushed, glass capillary. The unit cell parameters were obtained by the least-squares refinement of the angular settings of 24 reflections ($20° \le 2\theta \le 24°$). The systematic absences in the diffraction data are uniquely consistent for the reported space group. The structure was solved using direct methods, completed by subsequent difference Fourier syntheses, and refined by full-matrix least-squares procedures. Semiempirical absorption corrections were applied. All non-hydrogen atoms were refined with anisotropic displacement coefficients. Hydrogen atoms were treated as idealized contributions. The largest remaining peak in the difference map (1.29 e Å^{-3}) occurs at a chemically unreasonable position and was considered to be noise. All software and sources of the scattering factors are contained in the SHELXTL PLUS (4.2) program library (G. Sheldrick, Siemens XRD, Madison, WI). Crystal, data collection, and refinement parameters are given in Table 1.

X-ray Crystal Structure Determination of 5b. The crystal structure of **5b** was obtained at 173 K on a Siemens R3m/V diffractometer fitted with a Nicolet LT-2 low-temperature device. A suitable crystal of dimensions 0.46 × 0.44 × 0.58 mm was coated with Paratone oil (Exxon) and mounted under a stream of nitrogen. The unit cell dimensions were calculated from the angular settings of 47 reflections located from a rotation photograph and an automatic peak search routine. **5b** was found to crystallize in the monoclinic system. A total of 5343 reflections were collected using ω-scans, of which 5024 were determined to be unique. Corrections for Lorentz and polarization effects were made during data

Scheme 1

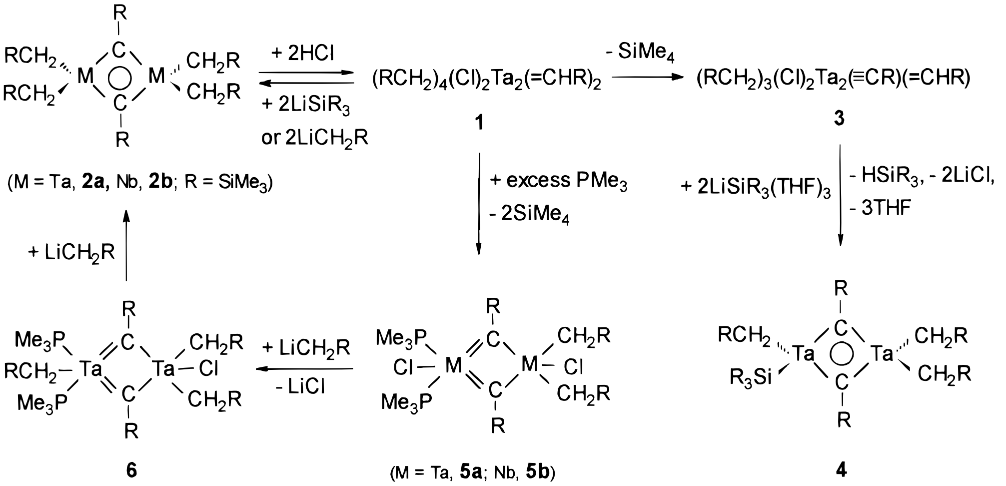

reduction, and an absorption correction based on ψ-scans collected on 5 reflections with $14° < 2\theta < 36°$ was applied. The $|E^*E-1|$ statistics, as well as the observed systematic absences, were uniquely consistent with the space group $P2_1/n$. The structure was solved using the Siemens SHELXTL 93 (Version 5) proprietary software package. The niobium atoms were found by the Patterson method. The structure was completed by successive Fourier syntheses and refined to convergence by successive full-matrix least-squares refinements of F^2. All non-hydrogen atoms were anisotropically refined. The hydrogen atoms were placed in calculated positions and introduced into the refinement as fixed contributors with isotropic U values of 0.08 Å^2. Crystal, data collection, and refinement parameters are given in Table 1.

Results and Discussion

The reactions leading to the formation of products **1** and **3**−**6** are shown in Scheme 1.

Synthesis of the Bis(alkylidene) Complex 1 and Its Conversion to the Alkylidene−Alkylidyne Complex 3. The addition of 2 equiv of HCl to $(RCH_2)_2Ta(\mu\text{-}CR)_2Ta(CH_2R)_2$ (**2a**) leads to almost quantitative formation of the thermally unstable bis(alkylidene) complex $(RCH_2)_4(Cl)_2Ta_2({=}CHR)_2$ (**1**). The two molecules of HCl were found to add to the Ta=C bonds instead of reacting with the Ta−CH_2R bonds to eliminate $SiMe_4$ (Scheme 1). **1** was found to decompose above −50 °C.

There are two possible structures for **1** that are consistent with its NMR spectra and reactivities. Complex **1** may contain either alkylidene (**1-A**) or Cl^- (**1-B**) as bridging ligands.[17] For structure **1-A**, the NMR spectra at −50 °C are consistent with a trans configuration of the two bridging alkylidene ligands in the dimetallacyclobutadiene moiety.[17] The presence of a center of inversion in the molecule makes the two α-hydrogen atoms of the two bridging alkylidene ligands magnetically equivalent as seen in the ^1H NMR spectra. However, there is no mirror plane passing through the molecule, thus making the α-hydrogen atoms in each of the two $-CH_2R$ ligands in **1-A** diastereotopic as observed in the ^1H NMR data. In a trans configuration with Cl^- as the bridging ligands (**1-B**) and the alkylidene ligands in axial positions, the α-hydrogen atoms of the $-CH_2R$ are diastereotopic, as there is no mirror plane passing through the molecule.

1 is an electron-deficient compound. The dative bonds formed by the lone-pair electrons on the bridging Cl^- ligands in **1-B** increase the electron count on tantalum to 12. In comparison, the metal atoms in **1-A** are 10-electron centers. Thus on these grounds, it seems likely that **1-B** is the preferred structure for this thermally unstable chloroalkylidene dimer. Such preferential halide-bridging structures in the presence of alkylidene ligands have been observed in $[Ta({=}CH^tBu)(PMe_3)Cl_3]_2$,[18a] $\{W[{=}C(CH_2)_4](OCH_2{}^tBu)_2Br_2\}_2$,[18b] and $[Re({\equiv}C^tBu)({=}CH^tBu)(NH_2R)Cl_2]_2$ (R = ^tBu, 2,6-$C_6H_3Me_2$).[5e] On the other hand, the formation of alkylidyne-bridged **5a** from **1** suggests that **1-A** is favored, as the conversion **1-A** → **5a** would not require ligand transfers between metal centers.

The first step in the thermal decomposition of the chloroalkylidene dimer $(RCH_2)_4(Cl)_2Ta_2({=}CHR)_2$ (**1**) is an α-hydrogen abstraction between an alkyl ligand and the α-hydrogen atom of an alkylidene ligand, leading to the formation of an alkylidyne ligand in an unusual dinuclear alkylidene/alkylidyne complex $(RCH_2)_3(Cl)_2Ta_2({=}CHR)({\equiv}CR)$ (**3**). High-oxidation-state d^0 alkylidyne complexes comprise a large and varied class of compounds.[5] However, there is no firm conclusion regarding the mechanistic pathways leading to the formation of archetypal alkylidyne complexes $(Me_3ECH_2)_3M{\equiv}CEMe_3$ (E = C, Si; M = Mo, W). α-Hydrogen abstraction is believed to be involved in the $M-CH_2EMe_3 \rightarrow M{=}CHEMe_3 \rightarrow M{\equiv}CEMe_3$ conversions in the

---

(17) For other bridging alkylidene ligands, see: (a) Hartner, F. W., Jr.; Schwartz, J.; Clift, S. M. *J. Am. Chem. Soc.* **1983**, *105*, 640. (b) Hursthouse, M. B.; Jones, R. A.; Abdul Malik, K. M.; Wilkinson, G. *J. Am. Chem. Soc.* **1979**, *101*, 4128. (c) Schrock, R. R.; Sharp, P. R. *J. Am. Chem. Soc.* **1978**, *100*, 2389. (d) Schmidt, G. F.; Muetterties, E. L.; Beno; M. A.; Williams, J. M. *Proc. Natl. Acad. Sci. U.S.A.* **1981**, *78*, 1318. (e) Müller, J.; Passon, B.; Pickardt, J. *J. Organomet. Chem.* **1982**, *228*, C51. (f) Isobe, K.; Okeya, S.; Meanwell, N. J.; Smith, A. J.; Adams, H.; Maitlis, P. M. *J. Chem. Soc., Dalton Trans.* **1984**, 1215. (g) Jones, R. A.; Wilkinson, G.; Galas, A. M. R.; Hursthouse; M. B.; Abdul Malik, K. M. *J. Chem. Soc., Dalton Trans.* **1980**, 1771.

(18) (a) Schrock and co-workers have reported several dimeric alkylidene complexes $[M({=}CH^tBu)LX_3]_2$ (M = Nb, Ta; L = a tertiary phosphine; X = Cl, Br). Neutron diffraction studies have shown that $[Ta({=}CH^tBu)(PMe_3)Cl_3]_2$ contains two bridging halide ligands. Schultz, A. J.; Williams, J. M.; Schrock, R. R.; Rupprecht, G. A.; Fellmann, J. D. *J. Am. Chem. Soc.* **1979**, *101*, 1593. Rupprecht, G. A.; Messerle, L. W.; Fellmann, J. D.; Schrock, R. R. *J. Am. Chem. Soc.* **1980**, *102*, 6236. (b) Youinou, M. T.; Kress, J.; Fischer, J.; Aguero, A.; Osborn, J. A. *J. Am. Chem. Soc.* **1988**, *110*, 1488.

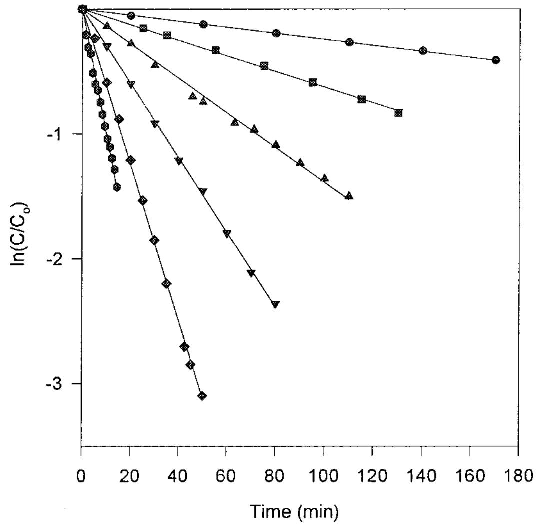

Figure 1. Kinetic plots of the decomposition of **1**.

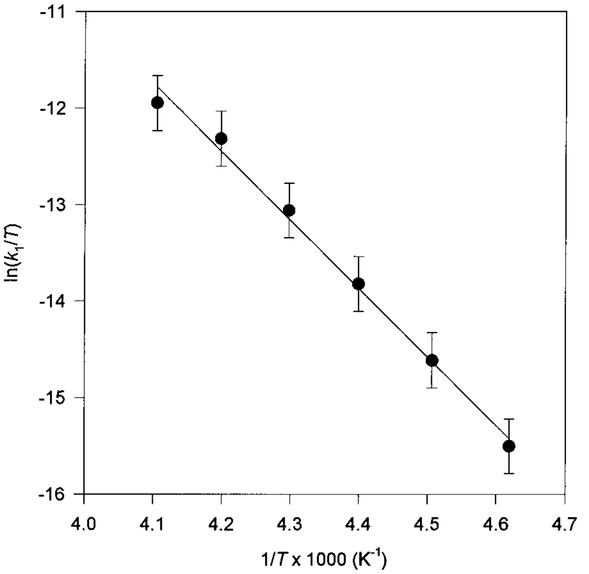

Figure 2. Eyring plot of the decomposition of **1**.

Table 2. Rate Constants k_1 for the Conversion 1 → 3[a]

T (K)	$(k_1 \pm \delta k_{1(\mathrm{ran})}) \times 10^4$ (s^{-1})
217 ± 1	0.400 ± 0.013
222 ± 1	0.996 ± 0.033
227 ± 1	2.25 ± 0.07
233 ± 1	4.95 ± 0.16
238 ± 1	10.7 ± 0.3
244 ± 1	15.8 ± 0.5

[a] The total uncertainty $\delta k_1/k_1$ of 6.0% was calculated from $\delta k_{1(\mathrm{ran})}/k_1 = 3.3\%$ and $\delta k_{1(\mathrm{sys})}/k_1 = 5\%$.[13]

Scheme 2. Proposed Mechanism for the Alkylidene to Alkylidyne Conversion in the Formation of 1 and 3

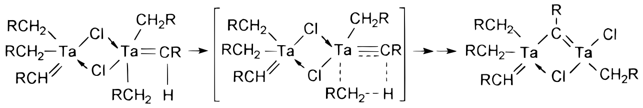

1-B **3-C**

formation of $(Me_3ECH_2)_3M{\equiv}CEMe_3$.[5] Earlier we reported a study of the conversion of an alkylidene complex $(RCH_2)_3Ta{=}CHR$ (R = $SiMe_3$) to the dimeric alkylidyne complex $(RCH_2)_4Ta_2(\mu\text{-}CR)_2$ (**2a**).[13] This conversion was found to follow second-order kinetics with a small activation enthalpy [$\Delta H^{\ddagger} = 6.2(0.3)$ kcal/mol] and a very negative activation entropy [$\Delta S^{\ddagger} = -61.6(0.8)$ eu].[13] To our knowledge, this was the only reported kinetic study of the alkylidene to alkylidyne conversion.[5] We thus decided to investigate, in the current study, the alkylidene → alkylidyne conversion in the formation of **3** from **1**. The elimination of $SiMe_4$ in this conversion was found to follow first-order kinetics. The kinetic plots and the Eyring plot are shown in Figures 1 and 2, respectively. The rate constants of the conversion **1** → **3** determined between 217 and 244 K are listed in Table 2. The activation enthalpy and entropy of this alkylidene to alkylidyne conversion thus calculated are $\Delta H_1^{\ddagger} = 14.1(0.8)$ kcal/mol and $\Delta S_1^{\ddagger} = -12(3)$ eu. The negative value for $\Delta S_1^{\ddagger}$ indicates a transition state where the rotation of bonds involved are restricted and the symmetry of the molecule descends. Such negative ΔS have been observed in C−H bond activation processes and are attributed to concerted four-center transition states, especially those involving cyclometalation.[19,20] The proposed reaction mechanism for the conversion of **1** → **3** is shown in Scheme 2. The kinetics and mechanism of this conversion are in contrast to those of alkylidene to alkylidyne conversion in the formation of dimeric **2a** from $(RCH_2)_3Ta{=}CHR$. The second-order kinetics observed in the $(RCH_2)_3Ta{=}CHR$ → **2a** conversion, the small activation enthalpy $\Delta H^{\ddagger}$, and the very negative activation entropy $\Delta S^{\ddagger}$ were attributed to dimerization of $(RCH_2)_3Ta{=}CHR$ as an integral part of the mechanism.[13]

To interpret the NMR spectra of **3**, we have considered five different isomers of **3** (Chart 2). The NOESY spectrum of **3** showed that (1) the $SiMe_3$ group on the alkylidyne (${\equiv}CSiMe_3$) ligand has NOE to five of the six $-CH_2-$ protons and (2) the $SiMe_3$ group on the alkylidene (${=}CHSiMe_3$) ligand has NOE to two protons on two different $-CH_2$ groups. On the basis of the NOESY spectrum, isomers **3-A**, **3-D**, and **3-E** may be ruled out. In the absence of structural information for **3**, we cannot distinguish between **3-B** and **3-C** by NMR. On the basis of electron count, **3-C** with a chloride bridge may be favored, as the dative bond by a lone electron pair on the chloride ligand alleviates electron deficiency in **3**. Such structures with preferential halide bridges have been reported.[5e,18a,b] As in the structure of **1**, the formation of alkylidyne-bridged **4** suggests that **3-B** with alkylidene−alkylidyne bridges is preferred, as the conversion **3-B** → **4** would not require ligand transfers between metal centers. In the assignment of the NMR

---

(19) For reviews of C−H activation by metal complexes, see, e.g.: (a) Rothwell, I. P.; *Polyhedron* **1985**, *4*, 177. (b) Shilov, A. E.; Shul'pin, G. B. *Chem. Rev.* **1997**, *97*, 2879.

(20) For activation parameters involving cyclometalation transition state, see, e.g.: (a) McDade, C.; Green, J. C.; Bercaw, J. E. *Organometallics* **1982**, *1*, 1629. (b) Bulls, A. R.; Schaefer, W. P.; Serfas, M.; Bercaw, J. E. *Organometallics* **1987**, *6*, 1219. (c) Vilardo, J. S.; Lockwood, M. A.; Hanson, L. G.; Clark, J. R.; Parkin, B. C.; Fanwick, P. E.; Rothwell, I. P. *J. Chem. Soc., Dalton Trans.* **1997**, 3353. (d) Rothwell, I. P. *Acc. Chem. Res.* **1988**, *21*, 153. (e) Smith, G. M.; Carpenter, J. D.; Marks, T. J. *J. Am. Chem. Soc.* **1986**, *108*, 6805. (f) Wood, C. D.; McLain, S. J.; Schrock, R. R. *J. Am. Chem. Soc.* **1979**, *101*, 3210. (g) Cheon, J.; Rogers, D. M.; Girolami, G. S. *J. Am. Chem. Soc.* **1997**, *119*, 6804. (h) Reference 13. (i) Caulton, K. G.; Chisholm, M. H.; Streib, W. E.; Xue, Z. *J. Am. Chem. Soc.* **1991**, *113*, 6082. (j) Buchwald, S. L.; Nielson, R. B. *J. Am. Chem. Soc.* **1988**, *110*, 3171. (k) Coles, N.; Harris, M. C. J.; Whitby, R. J.; Blagg, J. *Organometallics* **1994**, *13*, 190.

Chart 2. Five Possible Isomers of 3

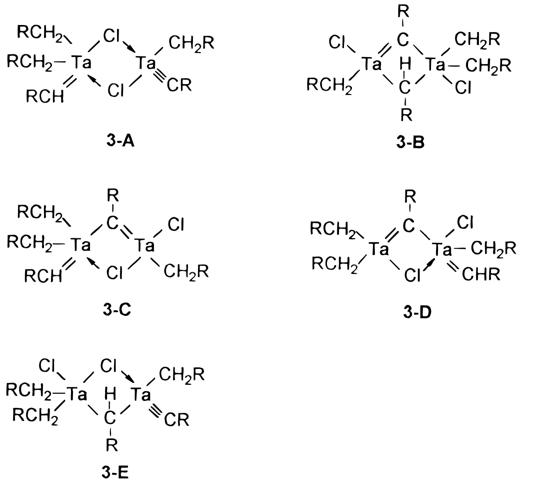
3-A 3-B 3-C 3-D 3-E

spectra of **3**, **3-C** was used (see Chart 1 and Experimental Section).

Synthesis and Structure of $(RCH_2)(R_3Si)Ta(\mu\text{-}CR)_2Ta(CH_2R)_2$ (4). This first silyl bis(alkylidyne) complex was prepared through the substitution of a chloride ligand in **3** by $LiSiR_3(THF)_3$. This Cp-free silyl complex is of particular interest. It is a silyl analogue of the archetypical alkyl bis(alkylidyne) compound $(RCH_2)_2Ta(\mu\text{-}CR)_2Ta(CH_2R)_2$ (**2a**),[6,21] and to our knowledge, it is the first structurally characterized d^0 silyl alkylidyne complex.

4 may be regarded as an adduct between "$(RCH_2)(R_3Si)Ta{\equiv}CR$" and "$(RCH_2)_2Ta{\equiv}CR$" through bridging alkylidyne ligands. The fact that this complex is dinuclear is consistent with what is observed for other structurally characterized alkylidyne complexes of tantalum[6,9,21] and indicates that the bulky $Si(SiMe_3)_3$ ligand is not sufficiently sterically demanding to result in the dissociation of **4** to a monomeric complex "$(RCH_2)(R_3Si)Ta{\equiv}CR$". In contrast, group 6 alkylidyne compounds such as $({}^tBuCH_2)_3W{\equiv}CSiMe_3$ are found to be monomeric.[20i] An ORTEP view of **4** is shown in Figure 3, and selected bond lengths and angles in **4** are shown in Table 3. The structure of this silyl bis(alkylidyne) **4** shares many features with that of its alkyl analogues **2a** and **2b**, which were first reported by Wilkinson and co-workers.[6,21] The two Ta−C(bridging) bond lengths are identical within estimated standard deviation; the average [1.9867(11) Å] is identical to that in **2a**. The Ta−Si bond length of 2.666(3) Å is comparable to other reported Ta−Si bond lengths. The two bridging carbon atoms and the Ta atoms are coplanar with a deviation of 0.001 Å, and the ring formed by these four atoms is quasi-aromatic. The Ta−Ta distance of 2.9 Å represents a nonbonding distance between the two metal atoms, and the Ta−C(bridging) bonds have multiple (e.g., 1.5) bond order. These bonding features can explain the diamagnetism of the complex.

Reactions of 1 with Lithium Silyl and Lithium Alkyl Reagents. Our original interest in preparing the dichloro bis(alkylidene) complex **1** was to use it as a starting material to prepare dinuclear silyl complexes. The addition of $LiSiR_3(THF)_n$ [$R_3 = (SiMe_3)_3$, $Ph_2{}^tBu$] to **1** did lead to the substitution of Cl^- ligands; however, subsequent α-hydrogen abstraction between the silyl and the alkylidene ligands led to the formation of **2a** (Scheme 1), $HSiR_3$, and a small amount of R_3SiSiR_3.[22] Alternatively the SiR_3^- anion may attack the alkylidene ligands directly to give **2a**. No other metal-containing species could be identified in the reaction mixtures. The reaction of **1** with $LiCH_2R$ similarly converted the bis(alkylidene) complex back to bis(alkylidyne) complex **2a**.

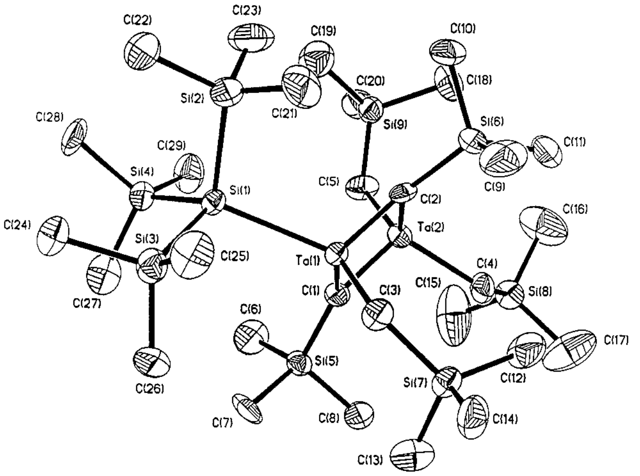

Figure 3. ORTEP drawing of **4** (thermal ellipsoids at the 35% probability level).

Table 3. Selected Bond Distances and Bond Angles in 4

Distances (Å)			
Ta(1)−C(1)	1.994(11)	Ta(1)−C(2)	1.979(11)
Ta(2)−C(1)	1.960(11)	Ta(2)−C(2)	2.020(10)
Ta(1)−Si(1)	2.666(3)	Ta(1)−C(3)	2.137(11)
Ta(2)−C(4)	2.157(12)	Ta(2)−C(5)	2.127(12)
C(1)−Si(5)	1.854(11)	C(2)−Si(6)	1.841(11)
Si(1)−Si(2)	2.337(5)	Si(1)−Si(3)	2.360(5)
Si(1)−Si(4)	2.340(5)		

Angles (deg)			
C(1)−Ta(1)−C(2)	87.1(4)	C(1)−Ta(2)−C(2)	86.9(4)
Ta(1)−C(1)−Ta(2)	93.7(5)	Ta(1)−C(2)−Ta(2)	92.3(4)
C(3)−Ta(1)−Si(1)	110.7(3)	C(4)−Ta(2)−C(5)	114.9(5)
Si(1)−Ta(1)−C(1)	112.8(3)	Si(1)−Ta(1)−C(2)	116.4(3)
C(3)−Ta(1)−C(1)	116.7(5)	C(3)−Ta(1)−C(2)	111.4(4)
C(4)−Ta(2)−C(1)	108.1(5)	C(4)−Ta(2)−C(2)	114.1(5)
C(5)−Ta(2)−C(1)	111.7(5)	C(5)−Ta(2)−C(2)	117.3(5)
Si(5)−C(1)−Ta(1)	134.0(7)	Si(5)−C(1)−Ta(2)	132.1(6)
Si(6)−C(2)−Ta(1)	137.3(6)	Si(6)−C(2)−Ta(2)	125.6(6)
Si(7)−C(3)−Ta(1)	132.3(6)	Si(8)−C(4)−Ta(2)	125.3(7)
Si(9)−C(5)−Ta(2)	129.6(7)		

Syntheses of the Nonsymmetric Bridging Bis(alkylidyne) Complexes 5a and 5b. A solution containing **1** was used in situ to prepare $(Me_3P)_2(Cl)Ta(\mu\text{-}CR)_2Ta(Cl)(CH_2R)_2$ (**5a**, Scheme 1). The analogous reaction between $(RCH_2)_2Nb(\mu\text{-}CR)_2Nb(CH_2R)_2$ (**2b**) and 2 equiv of HCl gave a mixture of thermally unstable products, which were used in situ to prepare $(Me_3P)_2(Cl)Nb(\mu\text{-}CR)_2Nb(Cl)(CH_2R)_2$ (**5b**). The addition of excess PMe_3 to a solution containing **1** (or the mixture from

---

(21) We have independently determined the structure of **2a**. A unit cell different from that reported in ref 6 was obtained. However there are no differences between the structure of **2a** and the reported structure of **2b**. Crystal data for **2a**, triclinic, $P\bar{1}$, a = 10.908(5) Å, b = 12.046 (4) Å, c = 16.134 (6) Å, α = 91.89 (3)°, β = 94.00 (3)°, γ = 115.67 (3)°, Z = 2, R = 0.0463, GOF on F^2 = 0.926.

(22) When the reactions were conducted in the presence of HSi^iPr_3 or H_2SiPh_2, no product of silane dimerization (${}^iPr_3SiSi^iPr_3$ or $Ph_2HSiSiHPh_2$) or crossover reaction ($Ph_2HSiSiR_3$ or ${}^iPr_3SiSiR_3$) was observed. The mechanism for the formation of a small amount of the disilane is not clear.

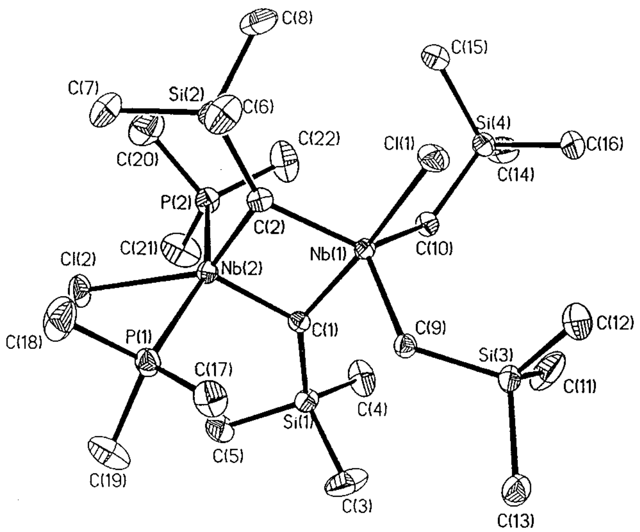

Figure 4. ORTEP drawing of **5b** (thermal ellipsoids at the 35% probability level). See ref 9 for an ORTEP drawing of **5a**.

the reaction of **2a** with 2 equiv of HCl) gave stable nonsymmetric bridging bis(alkylidyne) complexes **5a** and **5b** with the elimination of 2 equiv of $SiMe_4$ (Scheme 1). Interestingly the two PMe_3 molecules were added to one metal atom in these reactions, and no elimination or addition occurs on the other metal atom.

Crystal and Molecular Structures of 5a and 5b. An ORTEP view of **5b** is shown in Figure 4.[9] Selected bond distances and angles in **5a** and **5b** are given in Table 4. The isomorphous structures of **5a** and **5b** confirm the presence of nonsymmetric bis(alkylidyne) bridges; the bond distances between M(1) and the bridging alkylidyne atoms C(1) and C(2) [Ta(1), 2.099(6) and 2.073(6) Å; Nb(1), 2.098(3) and 2.052(3) Å, respectively] are significantly longer than those between M(2) and the bridging carbon atoms [Ta(2), 1.922(6) and 1.942(6) Å; Nb(2), 1.911(3) and 1.929(3) Å, respectively]. In comparison, the mean Ta−C(bridging) distances in the symmetric bis(alkylidyne) bridges in **2a** and **4** are 1.987 Å. The differences in the M−C bond distances (0.12−0.19 Å) for the nonsymmetrically bridging bis(alkylidyne) ligands in **5a** and **5b**, however, are smaller than those (0.33−0.48 Å) in the other known nonsymmetrically bridging bis(alkylidyne) complex $W_2(RCH_2)_4(\mu\text{-}CR)_2(\eta^2\text{-}PhC_2Me)$.[8] The M-to-M distances in **5a** and **5b**, 3.0 Å, represent nonbonding distances and are slightly longer than those (2.9 Å) observed in **2a**[6] and $W_2(RCH_2)_4(\mu\text{-}CR)_2(\eta^2\text{-}PhC_2Me)$.[8] The atoms Cl(1), M(1), C(1), C(2), M(2), and Cl(2) are virtually coplanar (deviations from the least-squares plane $\leq$ 0.07 Å, mean = 0.04 Å in **5a** and $\leq$ 0.09 Å, mean = 0.06 Å in **5b**, respectively). The two PMe_3 and two CH_2R ligands are thus chemically equivalent as seen in their ^1H, ^{13}C, and ^{31}P NMR spectra. The ligands on M(1) are arranged in a slightly distorted trigonal bipyramidal (TBP) geometry with C(1) and C(2) at axial and equatorial positions, respectively.

The largest bond angle on M(2) is P(1)−M(2)−P(2) (ca. 157°). The coordination on M(2) could be best described as a very distorted TBP with axial PMe_3 ligands and a constrained C(1)−M(2)−C(2) angle of ca. 89°. These constrained angles are the result of the bridging nature of these alkylidyne ligands. The structural features around M(2) are similar to those of monomeric $Ta(=CH^tBu)_2(mesityl)(PMe_3)_2$, which was reported by Schrock and structurally characterized by Churchill and their co-workers,[23] and $Ta(=CHR)_2(CH_2R)(PMe_3)_2$ (R = $SiMe_3$) that we reported recently.[4c] In these monomeric bis(alkylidene) complexes, both alkylidene ligands occupy the equatorial sites of the TBP.

Table 4. Selected Bond Distances (Å) and Bond Angles (deg) in 5A and 5b

	5a (M = Ta)	**5b** (M = Nb)
	Distances (Å)	
M(1)−C(1)	2.099(6)	2.098(3)
M(1)−C(2)	2.073(6)	2.050(3)
M(1)−C(9)	2.161(7)	2.180(3)
M(1)−C(10)	2.142(7)	2.152(3)
M(1)−Cl(1)	2.419(2)	2.4319(11)
M(2)−C(1)	1.922(6)	1.910(3)
M(2)−C(2)	1.942(7)	1.929(3)
M(2)−Cl(2)	2.465(2)	2.4845(11)
M(2)−P(1)	2.634(2)	2.6540(11)
M(2)−P(2)	2.633(2)	2.6611(11)
Si(1)−C(1)	1.844(7)	1.854(3)
Si(2)−C(2)	1.844(7)	1.861(3)
	Angles (deg)	
C(1)−M(1)−C(2)	81.3(3)	80.31(12)
C(1)−M(1)−C(9)	91.8(3)	89.74(12)
C(1)−M(1)−C(10)	93.3(3)	92.18(12)
C(2)−M(1)−C(9)	122.5(3)	121.23(12)
C(2)−M(1)−C(10)	122.4(3)	121.15(12)
C(9)−M(1)−C(10)	114.9(3)	116.96(12)
Cl(1)−M(1)−C(1)	172.2(2)	171.97(9)
C(2)−M(1)−Cl(1)	92.2(2)	94.13(9)
C(9)−M(1)−Cl(1)	88.1(2)	88.20(9)
C(10)−M(1)−Cl(1)	93.8(2)	95.68(9)
C(1)−M(2)−C(2)	89.4(3)	88.35(13)
M(1)−C(1)−M(2)	94.5(3)	95.16(13)
M(1)−C(2)−M(2)	94.8(3)	96.18(14)
Cl(2)−M(2)−C(1)	135.1(2)	135.63(10)
Cl(2)−M(2)−C(2)	135.5(2)	136.00(10)
P(1)−M(2)−C(1)	98.2(2)	97.88(10)
P(1)−M(2)−C(2)	97.9(2)	97.95(10)
Cl(2)−M(2)−P(1)	78.2(1)	77.97(4)
Cl(2)−M(2)−P(2)	79.0(1)	78.91(4)
P(2)−M(2)−C(1)	97.9(2)	98.70(10)
P(2)−M(2)−C(2)	98.4(2)	98.53(10)
P(1)−M(2)−P(2)	157.1(1)	156.88(3)
M(1)−C(1)−Si(1)	140.1(4)	141.7(2)
M(2)−C(1)−Si(1)	125.4(3)	123.1(2)
M(1)−C(2)−Si(2)	139.3(4)	139.2(2)
M(2)−C(2)−Si(2)	125.9(3)	124.6(2)

Chart 3

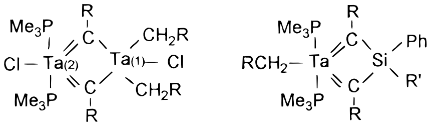

5a (R = $SiMe_3$) **7** (R' = Me, Ph)

The structural features around M(2) in **5a**,**b** also resemble those around the tantalum atom in novel 1,1′-metallasilacyclobutadiene complexes **7** (Chart 3), which we reported recently.[4e] Both complexes contain localized π-bonds in the 1,1′-metallocyclobutadiene moieties, and the two PMe_3 ligands in both complexes occupy the axial positions of the distorted TBP.

Axial−Equatorial Alkylidyne Ligand Exchanges in 5a and 5b. The two bridging alkylidyne ligands in

---

[23] (a) Fellmann, J. D.; Schrock, R. R.; Rupprecht, G. A. *J. Am. Chem. Soc.* **1981**, *103*, 5752. (b) Fellmann, J. D.; Rupprecht, G. A.; Wood, C. D.; Schrock, R. R. *J. Am. Chem. Soc.* **1978**, *100*, 5964. (c) Churchill, M. R.; Youngs, W. J. *Inorg. Chem.* **1979**, *18*, 1930.

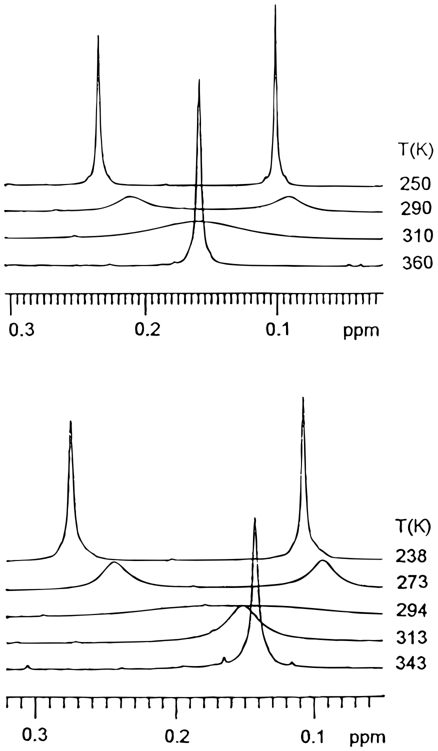

Figure 5. Variable-temperature ^{1}H NMR spectra (400.1 MHz) of the axial−equatorial alkylidyne ligand exchanges in **5a** (upper spectra) and **5b** (lower spectra).

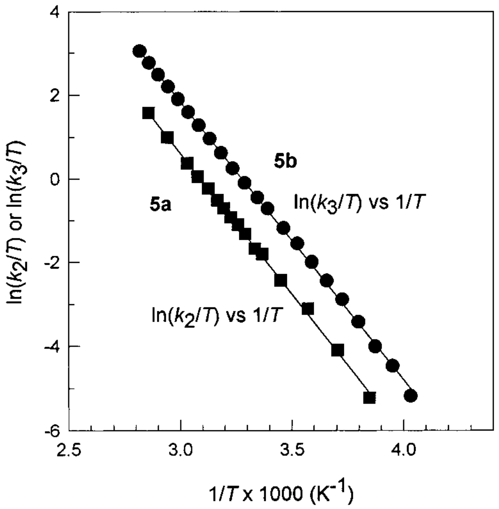

Figure 6. Eyring plots of the axial−equatorial alkylidyne ligand exchanges in **5a** and **5b**.

5a and **5b** are bonded to M(1) in axial and equatorial positions, respectively (Figure 4). They were found to be involved in an interesting axial−equatorial ligand exchange process (Scheme 3), as seen in the variable-temperature ^{1}H and ^{13}C NMR resonances of the $ME_3SiC\equiv$ groups (Figure 5). The exchange processes of the two complexes were found to have similar kinetics. Eyring plots of the exchanges are given in Figure 6. The activation enthalpies and entropies for the exchanges are $\Delta H_2^{\ddagger} = 13.6(0.4)$ kcal/mol and $\Delta S_2^{\ddagger} = -5(2)$ eu in **5a**, and $\Delta H_3^{\ddagger} = 13.0(0.3)$ kcal/mol and $\Delta S_3^{\ddagger} = -5(1)$ eu in **5b**. Exchange mechanisms such as Berry pseudorotation or trigonal twist may contribute to the observed dynamic processes. Similar ligand exchanges have been observed in $W(CR^1R^2)(OCH_2{}^tBu)_3X$ and $WO(CH_2{}^tBu)_3(NR_2)$.[24]

Scheme 3. Axial−Equatorial Alkylidyne Ligand Exchange in 5a and 5b

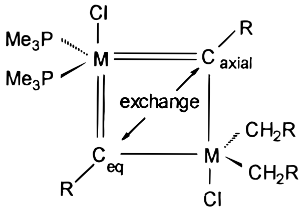

Reactions of 5a and 5b with Alkyl Lithium and Silyl Lithium Reagents. The reaction of **5a** or **5b** with 2 equiv of RCH_2Li led to the replacement of the two chloride ligands and the conversion of **5a** or **5b** back to the symmetric bis(alkylidyne) complex **2a** or **2b**, respectively, with elimination of two PMe_3 ligands (Scheme 1). The first RCH_2 substitution was found to occur at the Ta atom containing two PMe_3 ligands. A thermally unstable intermediate, $(Me_3P)_2(RCH_2)Ta(\mu\text{-}CR)_2Ta(Cl)(CH_2R)_2$ (**6**), was identified by its ^{1}H and ^{13}C NMR and ^{1}H−^{13}C HETCOR spectra at −50 °C. The NMR spectra of **6** are comparable to those of **5a** at −30 °C and indicate that there are two nonsymmetrically bridging bis(alkylidyne) ligands in **6**. As observed in the structures of **5a** and **5b**, the two bridging carbon atoms, the two Ta and the Cl atoms, and the CH_2R ligand adjacent to the PMe_3 ligands in **6** are perhaps coplanar, thus making the two PMe_3 and the two remaining CH_2R ligands chemically equivalent. Subsequent CH_2R substitution of the remaining Cl ligand in **6** led to the formation of **2a**. The analogous reaction of **5b** with RCH_2Li was much faster, and no intermediates were identified. The reaction of **5a** and **5b** with RCH_2Li to form **2a** and **2b**, respectively, thus completes an interesting reaction cycle **2a** → **1** → **5a** → **2a**, as shown in Scheme 1.

The results discussed here demonstrate that Cp-free tantalum alkylidyne compounds readily form dinuclear complexes through alkylidyne bridges. In the presence of phosphine ligands, nonsymmetric alkylidyne bridges in **5a**,**b** and **6** are formed with the PMe_3-containing Ta atom relatively electron-rich (14 valence electrons) and the other Ta atom electron-poor (10 electrons). Symmetric alkylidyne bridges in **2a**,**b** and **4** may reflect the efforts by these compounds to alleviate electron deficiency on the 10-electron metal centers by forming dinuclear complexes. When the chloride ligands in nonsymmetric alkylidyne complexes **5a**,**b** are replaced by bulkier alkyl ligands CH_2R, PMe_3 ligands are removed to form symmetric alkylidyne complexes **2a**,**b**, giving an interesting example of a reaction cycle between symmetric bis(alkylidyne), bis(alkylidene), and nonsymmetric bis(alkylidyne) compounds.

Acknowledgment. We thank the National Science Foundation (CHE-9457368), DuPont Young Professor Award, Camille Dreyfus Teacher-Scholar Award, the donors of the Petroleum Research Fund, administered by the American Chemical Society, and Exxon Educa

---

[24] (a) Kress, J.; Osborn, J. A. *J. Am. Chem. Soc.* **1987**, *109*, 3953. (b) Le Ny, J. P. Thesis, ULP Strasbourg, 1984.

tion Foundation, the University of Tennessee [Faculty Research Award and Scholarly Activities Research Incentive Fund (SARIF)], for support of this research. The authors also thank Professor G. S. Girolami for providing results before their publication and Dr. J. Richard Cox for assistance.

Supporting Information Available: Complete lists of the crystallographic data for **4**, **5a**, and **5b** and the table of rate constants for the axial−equatorial alkylidyne ligand exchanges in **5a** and **5b** (24 pages). See any current masthead page for ordering information and Web access instructions.

OM980652K